International Journal of Heat and Mass Transfer 65 (2013) 451–459

Contents lists available at SciVerse ScienceDirect

International Journal of Heat and Mass Transfer

journal homepage: www.elsevier.com/locate/ijhmt

Understanding transport mechanism of a self-sustained thermally driven oscillating two-phase system in a capillary tube

Manoj Rao [a,b,c], Frédéric Lefèvre [a,b,c], Sameer Khandekar [d,*], Jocelyn Bonjour [a,b,c]

[a] Université de Lyon, CNRS, France
[b] INSA-Lyon, CETHIL, UMR5008, F-69621, Villeurbanne, France
[c] Université Lyon 1, UMR5008, CETHIL, F-69622, France
[d] Department of Mechanical Engineering, Indian Institute of Technology Kanpur, Kanpur 208016, India

ARTICLE INFO

Article history:
Received 11 March 2013
Received in revised form 17 May 2013
Accepted 29 May 2013

Keywords:
Pulsating heat pipe
Oscillating meniscus
Non-equilibrium states
Scaling
Transient modeling

ABSTRACT

This paper makes an attempt to explain the self-sustained thermally-induced oscillations of a two-phase system consisting of an isolated confined liquid–vapor meniscus (a single liquid plug adjoining a vapor bubble) inside a circular capillary tube, the tube length being exposed to a net temperature gradient, thereby creating a continuous cycle of evaporation and condensation, leading to thermally induced auto-oscillations of the meniscus. This system represents the simplest 'unit-cell' version of a pulsating heat pipe (PHP). The fundamental understanding of its transport behavior leading to self-sustained oscillations is vital for building the hitherto non-existent mathematical models of the complete PHP system. First, visualization of the oscillations of the unit-cell has been done under controlled thermal boundary conditions. Here, a unique and novel understanding of the system dynamics has been achieved by real-time synchronization of the internal pressure measurement with high-speed videography. The contact angle hysteresis at the three-phase meniscus contact line during its upward and downward stroke plays a significant role in evaporation and condensation dynamics. Contrary to obvious interpretations, maximum pressure in the vapor bubble is achieved in the downward stroke, rather than the upward stroke. Thus, the system dynamics cannot be compared with gas-compression cycles; the presence of vapor coupled with transient phase-change processes give rise to singular transport phenomena. Such an interpretation of the meniscus motion and the resulting pressure cycles has not been considered by any of the existing mathematical models of PHPs. By simple scaling arguments, it is demonstrated that there is a high probability of metastable states existing in the system, which essentially point towards considering non-equilibrium evaporation and condensation models for predicting the thermal transport. A simple transient analytical model of thermal transport in the liquid film is developed which clearly explains the observed behavior. Existence of non-equilibrium conditions and there underlying effects on system dynamics need further exploration, both experimentally as well as analytically.

1. Introduction

A pulsating heat pipe (PHP) is an apparently simple looking heat transfer device, however with complex internal thermo-hydrodynamic transport processes, responsible for the self-sustained thermally driven oscillating two-phase Taylor bubble flow, which in turn, leads to its unique heat transfer characteristics. Research on PHP has received substantial attention in the recent past, due to its unique operating characteristics and potential applications in many passive heat transport situations [1–4]. A PHP consists of a simple capillary tube, with no wick structure, bent into many turns, and partially filled with a working fluid (for constructional details, refer to [4]). When the temperature difference between the heat source and the heat sink exceeds a certain threshold, the vapor bubbles and liquid plugs present inside the capillary tube begin to auto-oscillate back and forth. Heat is thus passively transferred, not only by latent heat exchange like in conventional wicked heat pipes, but also by sensible heat transfer between the wall and the fluid [5–8]. No external power is required to drive the device, internal oscillations being fully driven by the existing thermal non-equilibrium which is sustained inside the system due to external heating and cooling.

Compared to other passive heat transfer solutions, PHPs are quite simple in construction, and thus, more reliable and cheap. However, at present there are no theoretical models or correlations available that can predict the thermo-hydrodynamic transport behavior of PHPs. This prevents the widespread use of PHPs in industrial applications. Comprehensive and reliable mathematical design tools can only be formulated if the nuances of its operating

* Corresponding author. Tel.: +91 512 259 7038; fax: +91 512 259 7408.
E-mail address: samkhan@iitk.ac.in (S. Khandekar).

0017-9310/$ - see front matter © 2013 Elsevier Ltd. All rights reserved.
http://dx.doi.org/10.1016/j.ijheatmasstransfer.2013.05.067

Nomenclature

A_n	coefficients in the Fourier series (–)
h_{lv}	latent heat (J/kg)
k	thermal conductivity (W/m K)
$\overline{M}$	molecular weight (kg/mol)
P	pressure (Pa)
q''	heat flux (W/m^2)
$\overline{R}$	universal gas constant (J/mol K)
t	time (s)
T	temperature (°C or K)
x	coordinate (–)
X	location of the liquid–vapor interface (m)
Greek symbols	
α	thermal diffusivity (m^2/s)
δ	length scale (m)
ρ	density (kg/m^3)
$\hat{\sigma}$	accommodation coefficient (–)
Subscripts	
cond	condenser
f	fluid, film
i	interfacial
l	liquid
res	reservoir
sat	saturation
v	vapor
w	wall

principles are well understood, which, at present, remain rather inadequate. In this context, several authors have focused their efforts on understanding the simplest possible PHP structure, consisting of one liquid plug and one vapor bubble, also termed as a 'unit-cell'. Simplistic mathematical models based on the balance equations for such a simple unit-cell system have been presented [5,6,9,10]. The vapor-phase was considered as an ideal gas. The pressure fluctuations inside the system was introduced by modeling the evaporation of a thin liquid film left on the wall when the liquid plug leaves the evaporator. Recently, the first experimental results of such a system consisting of a 2.0 mm ID capillary tube, heated on one hand and cooled on the other end, were presented by Das et al. [11]. They were able to obtain thermally driven auto-oscillations in such a 'unit-cell' system under a definite range of operating experimental conditions. Temporal variation of vapor pressure was recorded. The passive thermally driven auto-oscillations of the liquid plug were observed; however, the visualization was restricted to only the condenser section. There were some important limitations with the approach of Das et al., which are listed herein:

(i) Experiments were done without any synchronization of the internal pressure measurements with the videography. As will be discussed subsequently, this led to serious shortcomings in the interpretation of the results.
(ii) For modeling the internal oscillatory phenomena of the meniscus existing between the vapor bubble and the liquid plug, they introduced an improved and coherent 'evaporation/condensation' model, as against the earlier simplified 'superheated vapor models' [5,6,9,10]. While this improvement could indeed predict the large amplitude oscillations observed in their experiments, the possibility of metastable conditions and/or non-equilibrium heat transfer of the liquid thin film were not considered by them.
(iii) The experimental setup was not fully transparent. The evaporator, made of copper, was opaque, and therefore the internal hydrodynamic phenomena could not be observed in totality; only, the condenser section was visible. This restricted data interpretation.
(iv) The connection between the opaque metal evaporator and the adiabatic section/condenser which was made of glass, presented several flow perturbations that might have disturbed the smooth meniscus movement to a certain extent.

In this background, this paper presents novel experimental data obtained with an improved version of the test bench, as was originally proposed by Das et al. [11], overcoming all its limitations listed above. The primary objective of this study is to enhance the fundamental understanding of the phenomena guiding the self-sustained thermally-induced two-phase oscillatory flows in the capillary tube of PHPs. Compared to the previous set-up of Das et al. [11], the new design of the experimental bench is entirely transparent in order to comprehensively observe the liquid film dynamics not only in the condenser, but also in the evaporator section too. Furthermore, the capillary tube is placed in a vertical heater-up position, intentionally providing the most unfavorable and demanding conditions for PHPs to operate. In the setup by Das et al. [11], the capillary tube was oriented in a horizontal position. Furthermore, the present set-up utilizes a seamless tube connection between the condenser and the evaporator sections, thus completely avoiding any flow perturbations due to geometrical or constructional singularities. Last but not the least, the pressure measurements are now fully synchronized in real-time with the high speed videography camera. This singular improvement of the setup has led to a drastic improvement in the overall understanding of the complex thin-film evaporation and ensuing pressure fluctuations inside the unit-cell. In fact, as will be explained later, some of the interpretations are so unique that it is likely to catalyze a new perspective in mathematical description of the phenomena.

2. The unit cell experiment

2.1. Experimental set-up

The experimental set-up is presented in Fig. 1. As noted, it is an improved version of a previous experimental design presented by Das et al. [11]. It mimics the basic unit-cell of a PHP, as detailed in Fig. 1, with one liquid plug and one vapor bubble, located in a vertical capillary tube of circular cross-section. The transparent capillary tube of inner diameter 2.0 mm, made of glass, is closed at one side and connected to a reservoir maintained at a constant pressure at the other side. The liquid plug oscillates between a heat source located near the upper closed side (evaporator section length = 10 cm) and a heat sink located near the bottom reservoir (condenser section length = 20 cm). In between, a small adiabatic section of length 1 cm separates the condenser and the evaporator. The evaporator and the condenser are transparent glass tube heat exchangers, whose temperature is controlled by two thermostatic baths. A third thermostatic bath is used to control the temperature of the reservoir, and thus its saturation pressure.

The two-phase oscillatory flow is characterized by vapor pressure measurements as well as meniscus displacement measurements. An absolute pressure sensor (supplied by Kistler®,

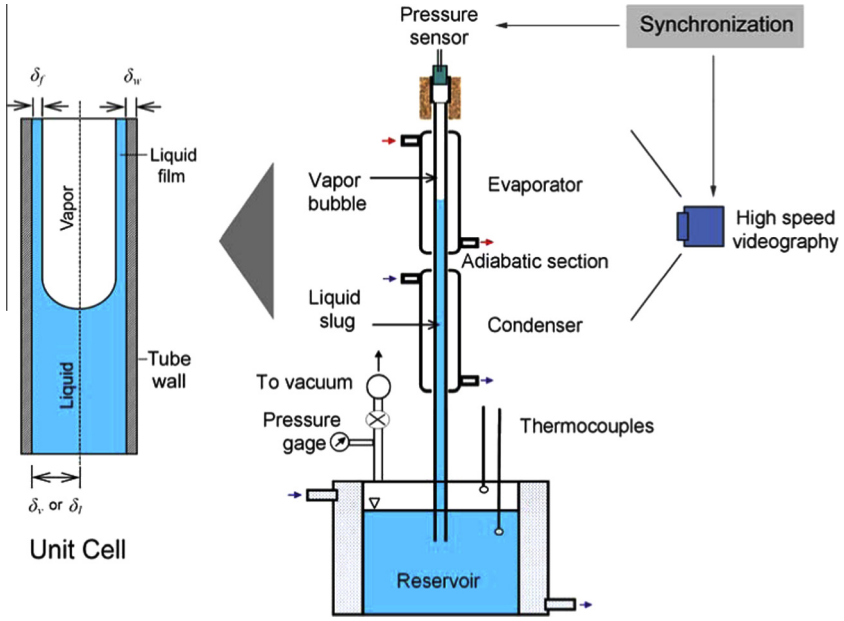

Fig. 1. Schematic of the experimental set-up for generating self-sustained thermally driven oscillating flow of 'unit-cell' consisting of one vapor bubble and one liquid plug. The details of the unit-cell highlighting the characteristic length scales of its four constituent elements are shown alongside (see Table 1 for typical order of magnitude of these length scales).

piezo-resistive sensor type 4005B, operating range of 0–5 bar) is located at the closed end of the tube and a high speed camera (Fastcam®-1024 PCI, 3000 fps) is used to record the meniscus displacement. The pressure sensor and the high speed camera are synchronized (in real-time domain) using the trigger function of the LabView® software. The trigger to start the acquisition from camera also simultaneously triggers the pressure sensor. Using this synchronization we get specified pressure value for particular location of the meniscus inside the tube. In this way, a direct one-to-one correspondence between the local pressure and the meniscus spatial position is established.

Prior to the experiments, the system is completely evacuated to remove the non-condensable gases with absolute pressure less than 10^{-4} Pa. The reservoir is then filled with the working fluid, i.e., FC72. The volume of the liquid reservoir is exceedingly large as compared to that of the capillary tube. This ensures that any internal meniscus oscillations have a negligible effect on the reservoir static pressure. The capillary tube always remains dipped inside the liquid irrespective of level of liquid in it. The changing in level affects the hydrostatic pressure at the outlet of the tube, but in third place of decimal, as the height of liquid above the tube exit is designed to be lower than 10 cm.

2.2. Transport mechanism

Fig. 2 shows a typical cycle of pressure variation in the system. The temperature of the evaporator and condenser are equal to 55 °C and −3 °C respectively. The reservoir pressure P_{res} is equal to 0.42 bars. Points of interest, with reference to the meniscus location are marked from A to G. Corresponding photographs of the meniscus in the downward and the upward stroke inside the evaporator section are shown in Fig. 3. A brief description of the phenomena, as observed in the system during the oscillation of the meniscus is as follows:

- Point A: At this point, the meniscus is at the highest position in the evaporator. It is important to note that the system pressure is not the highest at this point, in spite of the topmost meniscus location.
- Point B: At this point, the downward motion of the meniscus commences. Momentarily, between the point A and B, the meniscus dwells near the topmost position before beginning to move downwards.
- Point C: The meniscus is moving downwards and accompanying videos show rapid evaporation of the thin film (see Fig. 2a) which is formed due to the downward receding motion of the meniscus. As can be seen, this downward motion of the meniscus and the accompanying rapid evaporation of the thin liquid film results in a rapid pressure increase. The pressure-increase takes place due to the high rate of evaporation, and the resulting, vapor-mass addition, in the confined vapor space. The interplay of liquid plug inertia vis-à-vis rate of vapor addition due to evaporation leads to an increase of pressure in the vapor space.
- Point D: As point D approaches, the meniscus is just about to leave the evaporator area. No sooner the meniscus goes into the condenser, the vapor comes in contact with the cold condenser walls and this is accompanied by rapid depressurization of the vapor space due to condensation on internal tube wall surface.
- Point E: Here, the meniscus reaches the bottom-most location in the condenser while the condensation in the vapor space still continues. The depressurization in the vapor space now causes an upward force which eventually overcomes the inertia of the liquid plug and the meniscus starts its upward journey between point E and F.
- Point F: Now the meniscus is crossing over from the condenser to the evaporator region in its upwards journey. From here on, the vapor space gets cut-off from the cold condenser walls and is only interacting with the hot evaporator walls. Therefore, the upward motion of the meniscus is now able to compress the vapor and pressure in the vapor space rises from point F to point G.
- Point G: The meniscus is in the upward journey, the vapor space is getting compressed and the meniscus is in the process of approaching the topmost position in the evaporator. It should be noted that in the upward motion of the meniscus the dynamic contact angle which is made by the liquid with the wall is rather flat and no thin film can be seen. As the meniscus starts moving upwards, it first consumes the remnants of the earlier thin film which was formed in the

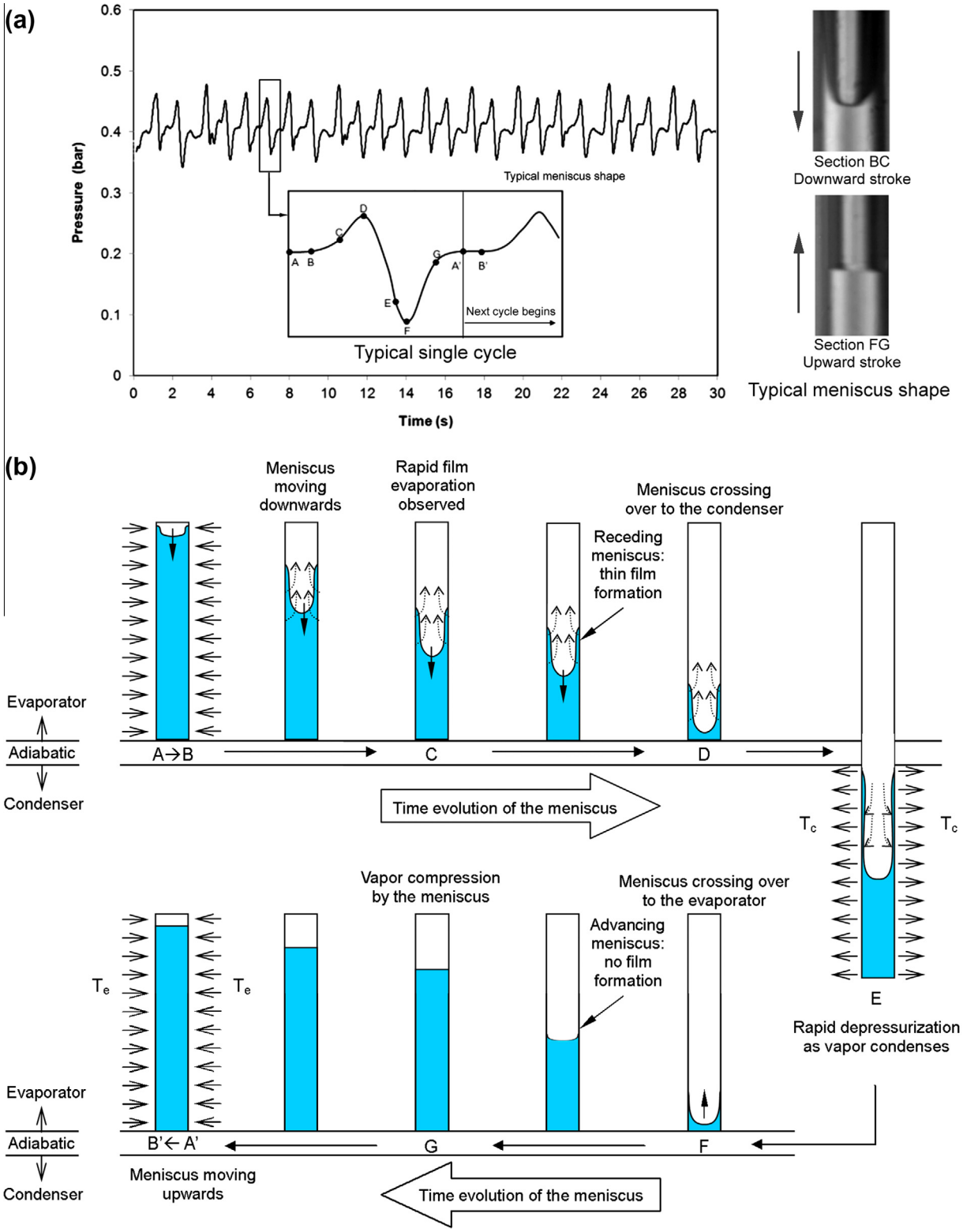

Fig. 2. (a) A typical temporal variation of pressure in the vapor bubble depicting several cycles of the meniscus (working fluid: FC72). The inset shows major stages in one cycle (A–G); typical photographs of the meniscus in the upward and downward motion are shown alongside; (b) Schematic explaining the events during one cycle of the meniscus motion. Time evolution of the meniscus from the evaporator top end (Stage A) as it passes towards the condenser (Stage E) and comes back to the evaporator (Stage A'), is shown.

downward motion of the meniscus, and then slowly flattens out (see Fig. 2a for details). Due to rapid change in the direction, the meniscus is seen to oscillate in the transverse direction as it emerges out of the condenser (Point F) before getting stabilized. From Point F to Point G, no explicit thin film formation is observed.

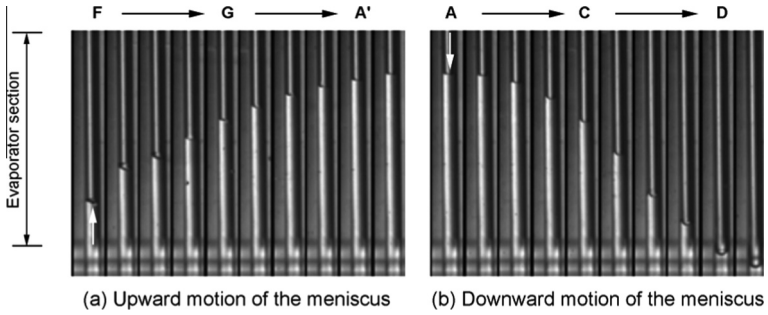

Fig. 3. Photographs of the meniscus in the downward and the upward stroke inside the evaporator section, corresponding to the time slots, as explained in Fig. 2.

- Points A' and B': These two points are identical to points A and B. The meniscus dwells at the topmost position for a very short time and then the cycle repeats itself.

3. Non-equilibrium states

3.1. Scaling arguments

It has been conjectured that non-equilibrium states of liquid and vapor are quite likely to exist during the operation of PHPs [8,12]. Conclusive experimental evidence is yet to come; it requires very precise and repeatable dynamic temperature measurements of local vapor and fluid film temperature so as to ascertain non-equilibrium condition and/or metastability. On one asymptote is the assumption that vapor and liquid in the Taylor bubbles are always under thermodynamic equilibrium. This essentially means that the relaxation time-scales of the phase-change by heat addition/subtraction are much faster than the typical characteristics time-scales of internal fluid flow and heat transfer through the walls in the PHP system. However, the essence of the entire PHP thermal phenomena lies in its transient characteristics. While one can talk about a 'quasi-steady' state in a global or lumped sense, nothing is, in fact, steady on the local level inside an operating PHP. Several experimental studies exist which indicate that the typical oscillating frequencies of the self-sustained thermally driven oscillations of a PHP are of the order of 0–5 Hz, which corresponds to fastest time scales of approximately 0.05 s or 0.1 s [13]. Statistically speaking, given the fact that the local thermodynamic quantities are changing continuously at this characteristic frequency at any given spatial location inside a PHP, the pertinent question to ask is, how different sub-constituents of the unit-cell respond to these changing thermodynamic conditions?

To answer this question, consider a typical PHP made up of copper tube of inside diameter 2.0 mm and outside diameter 3.0 mm, filled with water as the working fluid. Another example can be the glass tube PHP of the previous experiment with tube ID 2.0 mm and tube OD 6.0 mm, filled with FC72. For such a PHP, the unit cell may look, as depicted in Fig. 1. The four basic constituents of the unit cell, as depicted in the figure are as follows:

1. The vapor bubble.
2. The liquid film surrounding the vapor bubble.
3. The liquid plug adjacent to the vapor bubble.
4. The tube wall of the PHP.

Referring to Fig. 1, the characteristic length scale of the liquid slug (δ_l) and vapor bubble (δ_v), scales with the radius of the PHP tube, as a first order approximation. The characteristic length scale of the liquid film (δ_f) surrounding the vapor bubble can be estimated from any of the available popular correlations [14,15]. The characteristic length scale of the PHP tube (δ_w) scales with the tube thickness.

The thermal response of a material to a change in temperature is indicated by its thermal diffusivity. Fig. 4 compares the thermal conductivity to thermal diffusivity for a wide range of materials on a log–log scale [16]. The data points noted as condensed matter (liquids and solids) can be described as being near a straight line. As it can be noted, with respect to thermal diffusivity, gases are quite different as compared to the condensed matter. With respect to the transient nature of heat transfer in a PHP, it is worthwhile to note that all the three phases, viz. vapor phase, liquid phase and the solid phase (tube material), having drastically different thermal diffusivities are interacting with each other at all times. In fact, the difference in their respective thermal response, as against the inertia of the working fluid, eventually leads to the oscillating motion inside the device. Estimating the typical characteristics time scales of these three interacting sub-systems of the unit-cell will be of interest. Table 1 summarizes the typical values of the characteristic time scale and the corresponding characteristic frequency of response of the different elements of the unit-cell, as estimated for a copper tube filled with water and for the glass tube filled with FC72, as in the present experiment (see Fig. 1).

If the frequency of any external thermal change imposed on the boundary of these elements exceeds the respective characteristic frequency of the element under consideration, such perturbation information will, in principle, remain largely isolated from the concerned element of the unit-cell. Considering the fact that typical PHPs operate with dominant oscillating frequencies between 0 Hz and 5 Hz [13], several observations can be made by looking at the frequency estimates of Table 1:

- The liquid plug is the most sluggish in its response to any change in the external or internal thermal perturbations.
- The liquid plug response will be quite slow as compared to the liquid film surrounding the vapor bubble.
- The vapor space temperature change will be relatively quite fast and will largely follow the external imposed frequencies.
- The liquid thin film, as it thins down by evaporation or grows up by condensation, will respond extremely fast to the external stimuli of changing temperatures.

Table 1
Order of magnitude of important time scales of the unit-cell elements.

Length	Typical length scale (m)	Typical thermal diffusivity(m^2/s)	Characteristics time scale (s)	Characteristics frequency (Hz)
δ_l (FC72)	10^{-3}	3×10^{-8}	33	0.03
δ_l (H_20)	10^{-3}	1.5×10^{-7}	6.5	0.15
δ_f (FC72)	10^{-4}	3×10^{-8}	0.33	3
δ_f (H_20)	10^{-4}	1.5×10^{-7}	0.065	15
δ_v	10^{-3}	2×10^{-5}	0.05	20.0
$\delta_{w\text{-}copper}$	0.5×10^{-3}	1.1×10^{-4}	0.002	500
$\delta_{w\text{-}glass}$	2.0×10^{-3}	3.0×10^{-7}	12.0	0.08

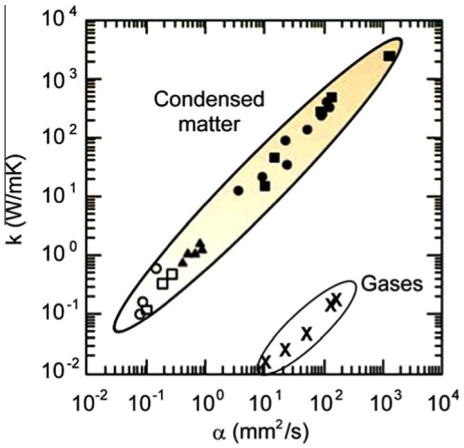

Fig. 4. Thermal conductivity versus thermal diffusivity for a wide variety of homogeneous materials (closed circles-metals; squares-ceramics; triangles-glasses; open squares-polymers; open circles-liquids; and crosses-gases) [16]

- There is a considerable difference in operating a PHP with glass tubes (representing low thermal conductivity materials) than metal tubes (high conductivity materials). This aspect has been neglected during data interpretation, in many of the earlier experimental studies.

Several other subtle issues get highlighted due to the order of magnitude difference in the characteristic time-scales of the constituents of the unit cell. For example, in a typical journey from the evaporator to the condenser, while the vapor will quickly respond to the change in temperature of its new colder surroundings, the liquid plug adjoining the vapor bubble will be much slower in loosing the sensible heat. From a thermodynamic standpoint, this essentially means that the probability of a temperature difference occurring between the liquid plug and the vapor bubble is quite high. In addition, there is considerable difference between the time response of the vapor and the surrounding liquid film. Thus, the very premise of the assumption of thermodynamic 'equilibrium', in the context of PHPs is rather misleading and inappropriate. In spite of the fact that explicit experimental evidence of non-equilibrium in PHP systems is yet to appear, the arguments presented above clearly indicate that the very nature of PHP heat transfer is guided by this inherent non-equilibrium existing between the vapor bubbles and adjoining liquid plugs. The system always tries to come to equilibrium locally by either exchanging heat/mass with the wall, or by exchanging heat/mass with the surrounding elements of the unit-cell with which a temperature difference exists so as to rearrange the respective chemical potentials of the two phases. Any change in the respective specific Gibbs free energy, due to a temperature or a pressure imbalance at the interface will lead to a driving potential for local phase-change. Moreover, change in temperature of the vapor can also take place by compression of its volume experienced via the movement of the adjoining liquid plugs. This local compression of a particular unit-cell can be an outcome of events taking place at other locations in the device. If such an event takes place in the adiabatic zone, the temperature of the vapor bubble will rise, depending on the adiabatic index of compression. In such a situation, if the process is fast enough, then there is more likelihood of the liquid film responding to the change in the vapor temperature than the adjoining bulk phase of the liquid plugs.

Considering the fact that non-equilibrium conditions exist inside the system, it is worthwhile to compare the heat transfer resistances experienced by the liquid film surrounding the bubble in getting the required heat of evaporation (or vice versa). In general, the liquid thin-film essentially interacts with two elements, the vapor bubble and the tube wall. In the adiabatic zone, it can exchange heat/mass to/from the vapor bubble. Inside the evaporator and the condenser, transport of heat can occur either with the wall or with the vapor bubble. As pointed out earlier, possibility of vapor bubble to have a higher temperature than the tube wall exists due to compression of its volume by the adjoining liquid plugs. In an analogous way, the vapor bubble can become cooler than the adjoining wall due to expansion.[1] This discussion suggests that, a situation wherein a gradient between the wall temperature T_w and the vapor temperature T_v is generated, with the liquid film existing at a different temperature T_f, should be occurring routinely in the transient operation of the PHP system.

3.2. Thermal response of liquid thin film

Let us consider the temperature in a cross-section of the tube between point states B and C (Fig. 2), wherein the downward motion of the meniscus has just commenced from the evaporator. As it has been clearly seen in the experiments and explained in the previous section, a thin liquid film is laid down and remains on the tube wall as the meniscus moves in the downward stroke. The liquid film is bounded by the tube wall on one side and compressed vapor on the other side, as detailed in the unit-cell description of Fig. 1.

Let us assume that the initial temperature of this film is equal to the temperature of the meniscus, which, in turn, can be considered as equal to the condenser temperature T_{cond} as a first approximation, since the time response of the liquid slug is very small compared to the frequency of the meniscus motion. At this very first moment, the liquid film is bounded by the wall at temperature T_w and the vapor at temperature T_v. From the wall side, the liquid film is heated by thermal diffusion due to the strong temperature gradient between the wall and the liquid film. This diffusional heating is not instantaneous, but depends on the thermophysical properties of the liquid film and is guided by the unsteady heat diffusion equation. On the other side of the liquid film, the strong temperature gradient expected between the vapor and the liquid is likely to induce instantaneous heat transfer between the vapor and the liquid film. While thermodynamic considerations are trying to push the system to local equilibrium, there is a strong interplay of kinetic transport limitations which induces heat and mass inertia, thereby creating or sustaining local non-equilibrium conditions. Whether the vapor will condense on the interfacial boundary with the thin liquid film or alternately, the liquid film will evaporate into the vapor space will also be guided by the local degree of superheating/subcooling vis-à-vis the instantaneous saturation pressure. For example, under a dynamic situation of meniscus motion in the downward stroke in the evaporator, the liquid film may receive thermal energy from the wall as well as the vapor, if the latter is condensing on it. Alternately, the heat received from the wall can evaporate the liquid thin film thereby adding additional mass to the vapor space.

In real time operation, it is indeed possible that due to local distribution/variation of liquid film temperature and vapor temperature respectively, while part of the liquid film experiences condensation, another part gets subjected to vaporization. Such an interfacial transport process suggests that individual fluxes for condensation and vaporization must be derived from kinetic theory considerations, wherein fluxes in each direction are

[1] While in the adiabatic zone, the adiabatic index of compression and expansion can be assumed to be valid for the vapor, it is not possible to ascertain the index of compression under diabatic conditions, in the evaporator or the condenser, wherein compression and/or expansion can take place simultaneously with heat addition/removal.

derived separately and results superimposed to obtain the net flux. A simple kinetic model as proposed by Schrage (as reviewed in [17]), assuming that both incoming and outgoing molecular fluxes have distinct temperatures and have a Maxwellian distribution, provides the heat transfer between the vapor (at temperature T_v) and the liquid–vapor interface (at temperature T_{lv}), as given by:

$$q_i'' = \hat{\sigma} \cdot h_{lv} \left(\frac{\bar{M}}{2\pi\bar{R}}\right)^{0.5} \left(\frac{P_v}{T_v^{0.5}} - \frac{P_{sat}(T_{lv})}{T_{lv}^{0.5}}\right) \tag{1}$$

where, $\hat{\sigma}$ is the accommodation coefficient. Following the sign convention of Carey [17], q'' is positive when condensation occurs and negative when vaporization occurs, which depends on the initial temperature of the liquid film. Due to the large difference of state between the vapor and the liquid when the liquid film is laid on the wall, considerably large heat transfer is expected to occur between the liquid film and the surrounding vapor. This relatively large energy exchange at the interface leads to increase or decrease of temperature in its vicinity, depending on whether local condensation or evaporation occurs. As the time response of the bulk liquid film is constrained by the heat diffusion equation, heat is stored or removed at the liquid–vapor interface until T_{lv} reaches the equilibrium state given by:

$$\frac{P_{sat}(T_{lv})}{T_{lv}^{0.5}} = \left(\frac{P_v}{T_v^{0.5}}\right) \tag{2}$$

If the initial temperature of the liquid film is lower than T_{lv}, condensation of vapor occurs as soon as the meniscus moves toward the condenser. Condensation process is replaced by vaporization when the heat coming from the wall reaches the liquid–vapor interface, enabling to change the temperature gradient at the interface. If the initial temperature of the liquid film is higher than T_{lv}, the temperature gradient enables the evaporation as soon as the liquid film is deposited on the wall. In both cases, the evaporation time is principally controlled by the heat diffusion equation in the liquid film, with two Dirichlet boundary conditions on each of its sides. Let us consider the one-dimensional unsteady state heat transfer equation in the liquid film:

$$\alpha \frac{\partial^2 T}{\partial x^2} = \frac{\partial T}{\partial t} \tag{3}$$

with the following boundary conditions:

$$T|_{x=0} = T_w \tag{4}$$

$$T|_{x=X(t)} = T_{lv} \tag{5}$$

where, $X(t)$ is the location of the liquid–vapor interface. Let us assume that the pressure and the temperature of the vapor are constant, which as a first approximation does not change the essence of the thin film evaporation. Thus, T_{lv} can also be considered as a constant. The location of the liquid vapor interface is given by the following boundary conditions:

$$-k \left.\frac{dT}{dx}\right|_{x=X(t)} = -h_{lv}\rho_l \frac{dX(t)}{dt} \tag{6}$$

The initial conditions for the thin film are the initial thickness δ_{f0} and the initial temperature field:

$$T(x,0) = T_{cond} \tag{7}$$

The method of separation of variables leads to the following solution for Eq. (3):

$$T(x,t) = \sum_{n=1}^{\infty} A_n e^{-\alpha\left(\frac{n\pi}{X(t)}\right)^2 t} \sin\left(\frac{n\pi x}{X(t)}\right) + \frac{T_{lv} - T_w}{X(t)} x + T_w \tag{8}$$

where,

$$A_n = \frac{2(T_{lv} - T_{cond})}{n\pi} \cos(n\pi) + \frac{2(T_{cond} - T_w)}{n\pi} \tag{9}$$

From Eq. (6), it is possible to derive the time variation of the thickness of the liquid film:

$$\left.\frac{dT}{dx}\right|_{x=X(t)} = \frac{h_{lv}\rho_l}{k} \frac{dX(t)}{dt} \tag{10}$$

where, the temperature gradient at the moving boundary is calculated from Eq. (8). Thus, the variation of the film thickness can be expressed as:

$$\frac{dX(t)}{dt} = \frac{k}{h_{lv}\rho_l} \left[\sum_{n=1}^{\infty} A_n e^{-\alpha\left(\frac{n\pi}{X(t)}\right)^2 t} \frac{n\pi}{X(t)} \cos(n\pi) + \frac{T_{lv} - T_w}{X(t)}\right] \tag{11}$$

Equation (11) is a non-linear first order differential equation of the location of the liquid–vapor interface. A time $t = 0$ s, the initial thickness of the film δ_{f0} is the inlet parameter of the model.

It has to be noted that the model can also be used in the condenser area to estimate the time scale of condensation. In that case, the temperature of the wall T_w is equal to T_{cond}.

3.3. Film thickness variation during phase-change

In this section, we present simulations obtained with the analytical model presented above for the experimental conditions, namely $T_w = 55$ °C, $T_{cond} = -3$ °C and $P_{res} = 0.42$ bars, with FC72 as the working fluid. The properties of FC72 are provided by the manufacturer of this fluid: 3M Company. Let us assume that the pressure of the vapor is equal to P_{res} as a first approximation. In reality, the vapor pressure fluctuates around this value during one cycle (Fig. 2). There are two main unknowns in the model: the initial thickness of the liquid film and the temperature of the vapor T_v, which is needed to calculate the liquid–vapor interface temperature T_{lv}. Let us assume that T_v ranges between T_w and T_{sat} (P_v). Within this range of vapor temperature, the interface temperature T_{lv} (Eq. (2)) is ranging between 33.2 °C and 34 °C. Thus, the superheating of the vapor does not have a strong influence on T_{lv} and we assume that T_v is equal to T_w in the following. Let us also assume that the temperature of the wall is equal to the temperature of the evaporator; the wall poses no thermal resistance.

Fig. 5 presents the temperature field of the liquid film at different times assuming an initial film thickness equal to 50 μm. The vapor initially condensates until time $t = 24$ ms, after which the temperature gradient inside the film becomes negative enabling the evaporation of the liquid thin film to begin. Till that time, the thickness of the film has increased to 58 μm due to mass addition when the vapor condensates. At time $t = 93$ ms, the thickness of the film reaches the initial thickness again, as a result of evaporation. Thus, a time delay of about 100 ms is necessary before the net evaporation of the film begins. This is not at all negligible since it represents 1/5th of the meniscus oscillation period. The liquid film gets totally evaporated at time $t = 0.25$ s, which represents about one half of the period.

Fig. 6 shows the variation of the liquid film thickness as a function of time in the same conditions corresponding to Fig. 5. One can clearly see two phases: the film thickness increases rapidly due to the large condensation rate which is initially prevalent. When the overall temperature of the film is close to T_{lv}, the thickness stabilizes until the evaporation of the film begins, the heat being now supplied from the elevated wall temperature. With the decrease of the film thickness, the thermal resistance decreases and therefore the evaporation rate increases, until the film completely disappears.

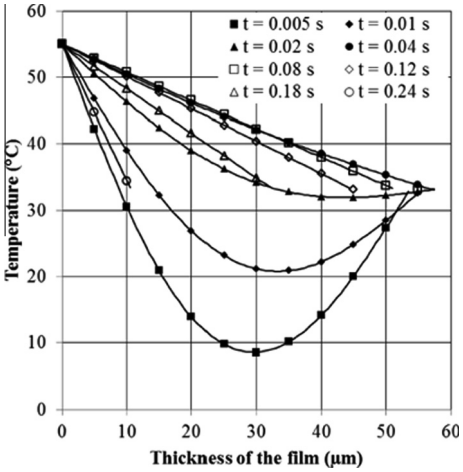

Fig. 5. Temporal variation of the liquid film thickness ($\delta_{f0} = 50$ μm) and its corresponding temperature at the conditions existing in the evaporator section of the present experiment.

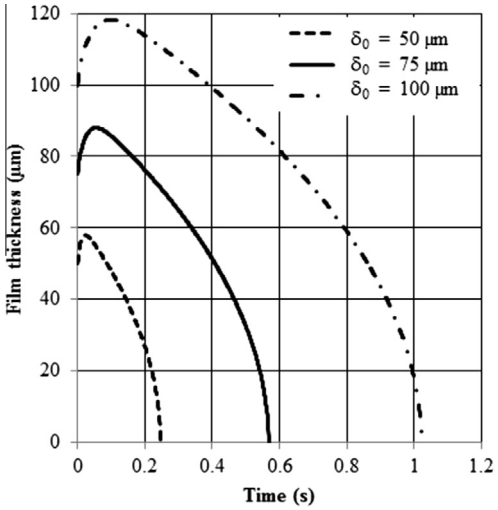

Fig. 7. Influence of the initial thickness of the liquid film on its evolution from initial condition to the final state of complete evaporation. During the initial period the film becomes thicker as it experiences condensation of vapor on it.

Fig. 7 shows the major influence of the film thickness on the time required to evaporate the film. Three initial liquid film thicknesses are compared: $\delta_{f0} = 50$ μm, $\delta_{f0} = 75$ μm and $\delta_{f0} = 100$ μm. Obviously, the time required to evaporate the film increases with the increase of δ_{f0}. The time period for which the initial phase of condensation prevails is equal to 24 ms, 54 ms and 100 ms, and the time period before net evaporation begins is equal to 93 ms, 210 ms and 390 ms for initial film thickness $\delta_{f0} = 50$ μm, $\delta_{f0} = 75$ μm and $\delta_{f0} = 100$ μm, respectively. For the two last film thicknesses, the delay induced by the condensation is not compatible with the present experiment as the frequency is equal to 2 Hz. The next meniscus cycle will commence before the liquid film fully evaporates. The results show that when the thickness of the film is doubled, the delay is multiplied by four. Thus, a very precise estimation of the initial liquid film thickness is required to accurately modeling the PHP behavior.

The primary physical mechanisms that control the thickness of the liquid film are similar to that encountered in dip-coating problems, wherein a solid substrate is withdrawn from a liquid bath, so as to deposit a liquid film on it. In the case of a PHP, the tube is stable and the liquid moves but the underlying principles are similar. These kinds of films are described as the Landau–Levich flows from the names of the two authors who first reported on this problem in 1942 [18]. It has been shown that the thickness of the film depends on several non-dimensional numbers like the Capillary number and the Capillary length scale [18]. The geometry of the substrate, as well as its wettability, are also important parameters. Literature related to dip-coating problems, an active field of contemporary research, needs to be explored for further understanding the consequence of wettability on internal film dynamics of PHPs and the eventual effect on thermal performance.

The model presented in Section 3 can also be used to study the heat transfer phenomena at the condenser. In that case, the temperature of the wall is set to the condenser temperature (e.g. −3 °C in the conditions of the experiment). Fig. 8 presents the temperature of the film for different times assuming an initial thickness of 50 μm. One can clearly see that the condensation rate is intense in the early stages and decreases subsequently as the film thickness increases. As the thermal resistance of the film increases, the condensation rate is lower than the evaporation rate. Nevertheless, as there is no delay at the condenser, at time $t = 0.25$ s (which corresponds to the time needed to evaporate a film of thickness 50 μm), the increase of the film thickness is equal to 50 μm at the condenser. Thus, the mean rate of condensation is equal to the mean rate of evaporation, but the dynamics of both

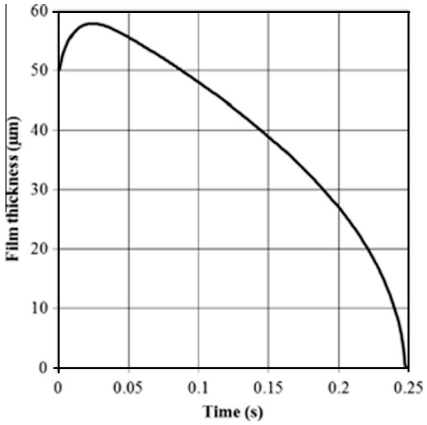

Fig. 6. Temporal variation of liquid film thickness ($\delta_{f0} = 50$ μm) at the conditions existing in the evaporator section of the present experiment.

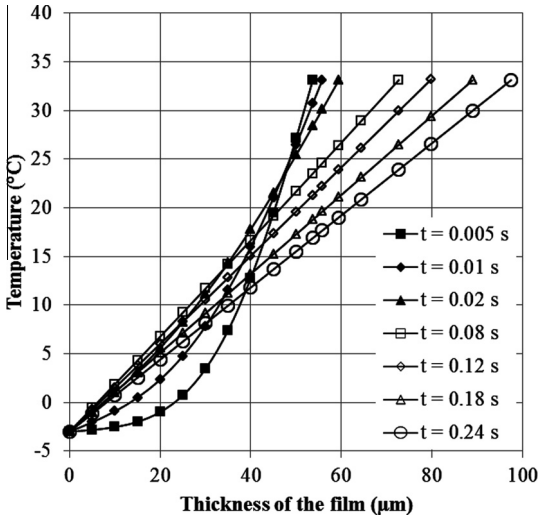

Fig. 8. Temperature of the liquid film ($\delta_{f0} = 50$ μm) at different time in the conditions of the experiment at the condenser.

heat transfer processes are different, condensation process being more regular.

This simple analysis can obviously not describe the entirety of the complex process of heat and mass exchange during the cycle of the vapor bubble–liquid slug interface in an operating PHP. For instance, the above analysis tends to show that during any portion of the cycle, when the meniscus is in the evaporator, the thinnest portion of the liquid film is subject to evaporation while the thickest portion of the film is simultaneously subjected to condensation (from the vapor) and evaporation (due to the heat flowing from the wall) that eventually results in net evaporation. Taking this observation into account, and the thermally thick character of the liquid film, it is imperative that a comprehensive treatment of the unit-cell is required for deeper understanding of the involved spatio-temporal phenomena. Alternately, just considering evaporation of the film is not sufficient, as part of the film may also be experiencing condensation due to the local spatial thermal non-equilibrium. From an experimental viewpoint, it is now clear that at least two new parameters should be measured as a function of time to describe quantitatively the mechanisms involved in the studied system: the time evolution of the vapor temperature and either the film shape/size or the time required for its evaporation. Proper video-recording could allow characterizing the film geometry and its time-dependant evolution, but measuring the vapor temperature with high time-resolution and with minimal perturbation certainly remains a challenge to be addressed in the future.

4. Summary and conclusions

- Self sustained thermally driven oscillations of a single meniscus can be obtained and efficiently sustained inside a capillary tube over long periods of time by maintaining a step thermal gradient over its length. Associated phase-change processes lead to thermo-mechanical instability in the system which generates the auto-oscillations of the meniscus.
- The demonstrated system manifests all the fundamental characteristics of the complex pulsating heat pipe device and can be effectively used to study its primary transport behavior from first-principles.
- The dynamic contact angle of the meniscus is totally different in the downward and the upward stroke. In the upward stroke, the receding dynamic contact angle of the moving meniscus is close to 90° and the vapor space gets compressed once the meniscus leaves the condenser. There is no thin film seen and no phase change.
- In the downward stroke, the meniscus shows strong curvatures and lays a thin liquid film along the tube inner wall. As the meniscus goes down the evaporator, there is a strong presence of evaporation. Thus, contrary to obvious but erroneous interpretation (which will come if the vapor space is modeled as an ideal gas), downward stroke of the meniscus (leading to an increase of internal volume of the vapor bubble) actually leads to an increase of the pressure inside the vapor space, due to rapid evaporation.
- The evaporation mass flux experienced in the vapor space is not only due to the heat flow by conduction from the wall to the interface, but also to the thermal non-equilibrium between the vapor and the liquid. If the vapor temperature is greater than the liquid temperature, the net mass flux of evaporation will be lower than conduction–induced evaporation mass flux, as the thermal non-equilibrium leads to condensation. Otherwise, the mass flux is due to both conduction through the film and thermal non-equilibrium.
- The simplified analysis of unsteady heat transfer in the liquid thin film shows the importance of measuring the time-evolution of the temperature of the vapor with a high time-resolution and a good accuracy, which remains a challenge today under such experimental conditions.

Acknowledgements

Financial support from the Indo-French Centre for the Promotion of Advanced Research, New Delhi (Project #: IFCPAR: 4408-1/2010), under the aegis of Indian Department of Science and Technology and the French Ministry of Foreign Affairs is gratefully acknowledged. Especially, part of this article was written during the scientific visit of Prof. Jocelyn Bonjour to IIT Kanpur under the financial support of CEFIPRA. In addition, Prof. Sameer Khandekar would also like to thank the administration of CETHIL – INSA de Lyon for extending invitation to him as a visiting research fellow during the summer of 2012. This work was also supported by the ANR in the frame of the TDM-AAP project "AARDECO".

References

[1] Y. Zhang, A. Faghri, Heat transfer in a pulsating heat pipe with open end, Int. J. Heat Mass Transfer 45 (2002) 755–764.
[2] L.L. Vasiliev, Heat pipes in modern heat exchangers, Appl. Therm. Eng. 25 (2005) 1–19.
[3] A. Bensalem, Contribution to the analysis of the behavior of oscillating heat pipe for space purpose by experimental and numerical means, Ph. D. Thesis, Université de Poitiers, France, (2008), available http://theses.edel.univ-poitiers.fr/index.php?id=330, accessed March 2013).
[4] S. Khandekar, V. Silwal, A. Bhatnagar, P. Sharma, Global effectiveness of pulsating heat pipe heat exchangers: modeling and experiments, Heat Pipe Sci. Technol. – Int. J. 1 (3) (2010) 279–302.
[5] M.B. Shafii, A. Faghri, Y. Zhang, Thermal modeling of unlooped and looped pulsating heat pipes, J. Heat Transfer 123 (6) (2001) 1159–1172.
[6] M.B. Shafii, A. Faghri, Y. Zhang, Analysis of heat transfer in looped and unlooped pulsating heat pipe, Int. J. Numer. Methods Heat Fluid Flow 12 (5) (2002) 585–609.
[7] S. Lips, A. Bensalem, Y. Bertin, V. Ayel, C. Romestant, J. Bonjour, Experimental evidences of distinct heat transfer regimes in pulsating heat pipes, Appl. Therm. Eng. 30 (2010) 900–907.
[8] S. Khandekar, M. Groll, An insight into thermo-hydraulic coupling in pulsating heat pipes, Int. J. Therm. Sci. 43 (1) (2004) 13–20.
[9] R.T. Dobson, Theoretical and experimental modelling of an open oscillatory heat pipe including gravity, Int. J. Therm. Sci. 43 (2) (2004) 113–119.
[10] R.T. Dobson, An open oscillatory heat pipe water pump, Appl. Therm. Eng. 25 (4) (2005) 603–621.
[11] S.P. Das, V.S. Nikolayev, F. Lefèvre, B. Pottier, S. Khandekar, J. Bonjour, Thermally induced two-phase oscillating flow inside a capillary tube, Int. J. Heat Mass Transfer 53 (2010) 3905–3913.
[12] M. Mameli, M. Marengo, S. Zinna, Thermal simulation of a pulsating heat pipe: effects of different liquid properties on a simple geometry, Heat Transfer Eng. 33 (14) (2012) 1177–1187.
[13] S. Khandekar, A.P. Gautam, P. Sharma, Multiple quasi-steady states in a closed loop pulsating heat pipe, Int. J. Therm. Sci. 48 (3) (2009) 535–546.
[14] P. Aussillous, D. Quéré, Quick deposition of a fluid on the wall of a tube, Phys. Fluids 12 (2000) 2367–2371.
[15] S. Khandekar, P.K. Panigrahi, F. Lefèvre, J. Bonjour, Local hydrodynamics of flow in a pulsating heat pipe: a review, Front. Heat Pipes 1 (2010). 023003(1–20).
[16] A. Salazar, On thermal diffusivity, Eur. J. Phys. 24 (2003) 351–358.
[17] V.P. Carey, Liquid–Vapor Phase-change Phenomena, second ed., Taylor and Francis, 2007.
[18] H.C. Mayer, R. Krechetnikov, Landau flow visualization: revealing the flow topology responsible for the film thickening phenomena, Phys. Fluid 24 (2012).